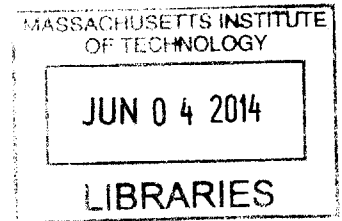# Swelling Properties of Hydrogel Coatings on Neural Devices

by
Di Judy Deng

Submitted to the Department of Materials Science and Engineering
in Partial Fulfillment of the Requirements for the Degree of **ARCHIVES**
Bachelor of Science
at the
Massachusetts Institute of Technology

© 2014 Di Deng
All rights reserved

The author hereby grants to MIT permission to reproduce and to distribute
publicly paper and electronic copies of this thesis document in whole or in
part in any medium now known or hereafter created

Signature redacted

Signature of Author ....
Department of Material Science and Engineering
May 2, 2014

Signature redacted

Certified by ....
Dr. Michael J. Cima
Professor of Engineering
Thesis supervisor

Signature redacted

Accepted by ....
Dr. Jeffrey C. Grossman
Undergraduate Committee Chair

Table of Contents

List of Tables

List of Figures

Abstract

Glial scarring is a major problem seen in brain electrode implants that can hinder electrode function. One major contributing factor is the mechanical mismatch between the stiff electrode and the soft brain tissue[i]. Hydrogel coatings are being investigated to determine their effectiveness in providing the necessary biocompatibility. Polyethylene glycol hydrogels of various formulations were fabricated and produced elastic moduli ranging from 13kPa to 687 kPa, which lie within two orders of magnitude of the elastic moduli of the brain (6kPa). Dehydration of the hydrogels provides the mechanical rigidity necessary for implantation into the brain. The surrounding aqueous environment allows the dried hydrogel to return to its swollen state. The swelling process in the brain phantom is slower than in unconstrained swelling. The equilibrium swollen hydrogel was also slightly smaller in the constrained state, implying the strain is being distributed between the hydrogel and the brain phantom.

1. Introduction

1.1. Significance

Errors in chemical and electrical signal transmissions can lead to miscommunication between different regions of the brain and cause circuit disorders. Treatments include deep brain stimulation, which has proven to be effective for several disorders. This surgical treatment allows scientists to electrically modulate and record brain activity in target regions by implanting an electrode into specific areas of the brain [i].

A large problem with device implantation into the brain is the brain tissue's response to these implants. Research has suggested that the surrounding tissue will initiate an inflammatory and wound healing response that is exacerbated over time as a result of the brain's micro-motions from everyday movement. A fibrous capsule develops over time that interferes with electrode and neuron cell body contact, which can negatively impact device function [ii].

Previous experiments have demonstrated a direct correlation between induced strains at the probe-tissue interface and the resultant scarring, suggesting mechanical mismatch to be a cause of scar formation [iii]. The elastic modulus of neural implants is often orders of magnitude larger than that of the brain. Borosilicate glass and the brain have elastic moduli of 69GPa and 6kPa, respectively. This mismatch causes the soft brain tissue to experience the majority of the strain. When the modulus of the implant is reduced, more strain will be shared between the device and the brain tissue. Subbaroyan et al showed through finite element analysis that reducing the moduli of the implant to the scale of megapascals can reduce the strain on the brain by two orders of magnitudes. This demonstrates a need for mechanical compatibility between the device and the brain tissue to minimize the brain's immune defenses and promote long-term usage of the device.

Coating neural probes with hydrogels is one potential approach to improve compatibility with brain tissue and reduce the strain caused by micro-motions. One problem with a coating is its adhesion strength to the capillary. Weak adhesion between the hydrogel and the capillary can damage the hydrogel during implantation. This thesis studies the effectiveness of using dehydration to preserve the hydrogel during implantation. It is hypothesized that a dehydrated hydrogel can be safely implanted and rehydrated from the high water content of the brain.

1.2. Hydrogels

Hydrogels are materials formed from a cross-linked network of polymer chains. A variety of hydrogels can be developed by manipulating the polymer composition and the cross-linking mechanism. Crosslinks can be formed through both chemical and physical means. The result is a hydrophilic material with unique mechanical and physical properties, including the ability to imbibe water and swell. Many hydrogels have been developed that are environmentally sensitive to factors such as pH, temperature, and ionic strength[iv]. Hydrogels are frequently used in bioengineering because they are easily modified and highly biocompatible.

One frequently used mechanism for forming crosslinks is photo-polymerization. The process utilizes light and photo-initiators to induce free radical polymerization of molecules. This method is beneficial because of its fast curing time, spatial and temporal control, and ability to be conducted in ambient temperatures. This allows for the formation of hydrogels on complex shapes, such as coatings on surfaces. The photo-polymerization process is initiated when a photo-initiator molecule is exposed to a specific wavelength of light and forms a radical species. The photo-initiator can be mixed into the hydrogel precursor solution

so that after activation, the radical species that are formed will cause the polymerization process to proceed throughout the bulk of the solution to form the hydrogel[iv] (Figure 1).

$$Rad^\bullet + H_2C = \underset{\underset{R}{|}}{CH} \longrightarrow Rad\text{-}CH_2 - \underset{\underset{R}{|}}{CH}^\bullet$$

$$Rad\text{-}CH_2 - \underset{\underset{R}{|}}{CH}^\bullet + H_2C = \underset{\underset{R}{|}}{CH} \longrightarrow Rad\text{-}CH_2 - \underset{\underset{R}{|}}{CH} - CH_2 - \underset{\underset{R}{|}}{CH}^\bullet$$
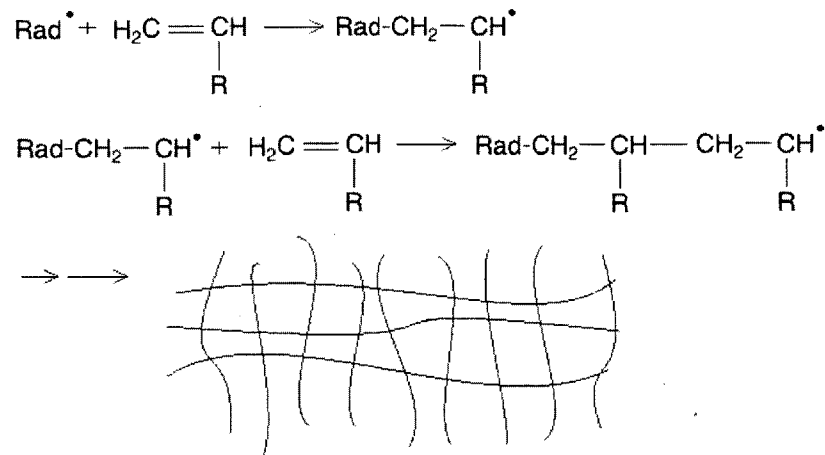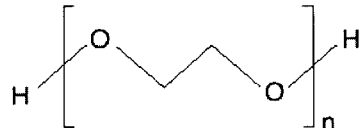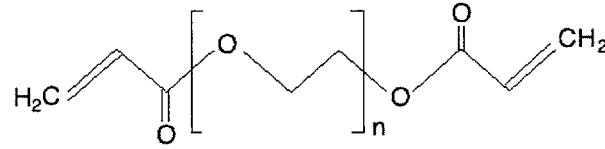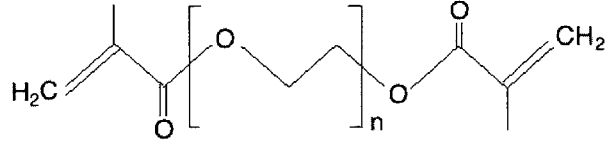
Figure 1. Photo-polymerization generates free radicals to initiate the polymerization process. Final representation of the hydrogel is idealized.

Polyethylene glycol (PEG) is a synthetic polyether that is biologically compatible due to its low toxicity and hydrophillicity. It is frequently used in vivo because it does not activate an immune response and prevents protein adhesion to surfaces. PEG chains can be easily functionalized with terminal acrylate groups to form PEG-diacrylate or PEG-dimethacrylate for cross-linking purposes[v] (Table 1).

Table 1

Structure of three forms of poly (ethylene glycol) polymers

Name	Structure
Poly(ethylene glycol)	
Poly(ethylene glycol) diacrylate	
Poly(ethylene glycol) dimethacrylate	

1.3. Hydrogel Swelling

A useful property of hydrogels is their ability to swell when placed in a thermodynamically compatible solvent. The tendency of systems towards higher entropy states drives the thermodynamic force of mixing, which causes the hydrogel to expand. The elastic force from the stretching polymer chains keeps the hydrogel together. The hydrogel will continue to imbibe the solvent until the increase in elastic energy of the chains balances the decrease in free energy from mixing. No additional swelling will occur and the hydrogel will stay at equilibrium. This effect is described the Flory-Rehner equation which can be rearranged to give an estimate of the average molecular weight between crosslinks[vi].

$$\frac{1}{\overline{M_c}} = \frac{2}{M_n} - \frac{\left(\frac{v}{V_1}\right)(\ln(1-v_{2,s})+v_{2,s}+\chi*v_{2,s}^2}{v_{2,s}^{1/3}-\frac{v_{2,s}}{2}} \tag{1}$$

9

where M_n is the number average molecular weight of the polymer chains, v is the specific volume of the bulk polymer in the amorphous state (0.893 cm^3/g)[vii], V_1 is the molar volume of the solvent (18 cm3/mole), χ is the polymer-solvent interaction parameter and $v_{2,s}$ is the polymer volume fraction in the swollen state.

The interaction parameter is relatively constant at $\chi = 0.426$ at room temperature for polymer volume fractions ranging from 0.04 to 0.2[viii]. The polymer volume fraction in the swollen state is a simple ratio of the volume of polymer to the total gel volume. It can be expressed in terms of the mass ratio and the densities of the polymer and solvent[iv].

$$v_{2,s} = \frac{v_p}{v_g} = Q_v^{-1} = \frac{1/\rho_p}{Q_m/\rho_s + 1/\rho_p} \qquad (2)$$

Q_m is the mass ratio or the swelling ratio and is defined as the mass of the gel over the mass of the polymer. The polymer volume fraction measures how much fluid can be taken up and retained by the hydrogel while the average molecular weight $\overline{M_c}$ between crosslinks is a measure of the degree of crosslinking.

A modified equation for the average molecular weight between crosslinks is used for hydrogels prepared in the presence of water. This altered equation takes into account the water-induced elastic contributions to swelling[vi].

$$\frac{1}{\overline{M_c^*}} = \frac{2}{M_n} - \frac{\left(\frac{v}{V_1}\right)\left(\ln\left(1-v_{2,s}\right)+v_{2,s}+\chi*v_{2,s}^2\right)}{v_{2,r}\left[\left(\frac{v_{2,s}}{v_{2,r}}\right)^{1/3}-\left(\frac{1}{2}\right)\left(\frac{v_{2,s}}{v_{2,r}}\right)\right]} \qquad (3)$$

The $v_{2,r}$ term is the volume fraction of the hydrogel in the relaxed state. This is the state of the hydrogel just after crosslinking but prior to being submerged in solvent to swell. The swelling ratio and the average molecular weight between crosslinks are the most useful values used to characterize hydrogel network structure.

10

1.4. Elastic Moduli

An elastic modulus for the hydrogel can be estimated using the rubber elasticity theory. This theory can be applied because up to deformations of 20%, hydrogels behave elastically and are capable of returning to their initial dimensions. The stress to a hydrogel sample[x] is

$$\tau = \frac{\rho RT}{M_c^*}\left(1 - \frac{2\overline{M_c}}{\overline{M_n}}\right)\left(\alpha - \frac{1}{\alpha^2}\right)\left(\frac{v_{2,s}}{v_{2,r}}\right)^{1/3} \qquad (4)$$

where α is extension parameter, or the final length over the initial length[ix]. This theory assumes Gaussian behavior of the polymer chains. The equation can be rearranged to solve for an approximation of the elastic modulus, which approaches a third of the Young's Modulus as the limit of α approaches 1^{ix}.

$$\frac{\tau}{\left(\alpha - \frac{1}{\alpha^2}\right)} = \frac{\rho RT}{M_c^*}\left(1 - \frac{2\overline{M_c^*}}{\overline{M_n}}\right)\left(\frac{v_{2,s}}{v_{2,r}}\right)^{1/3} \qquad (5)$$

2. Methods

2.1. Materials

Poly (ethylene glycol) diacrylate (PEG-DA) with a molecular weight of 700g/mole was obtained from Sigma-Aldrich (St. Louis, MO). Poly (ethylene glycol) dimethacrylate PEG-DM with molecular weights of 2000, 4000, 6000 and 8000 g/mole were synthesized using a published protocol[x]. Fluorescent and non-fluorescent Polybead® Polystyrene micro-particles of 6.0 μm were obtained from Polysciences, Inc. (Warrington, PA). All other reagents and chemicals, unless specifically mentioned were obtained from Sigma-Aldrich (St. Louis, MO).

2.2. Preparation of Hydrogel

The hydrogel precursor solution was produced from a mixture of either form of PEG, de-ionized (DI) water and photo-initiator. The PEG was dissolved in DI water to form concentrations of 5, 10 and 20% m/v PEG. The photo-initiator, 2-Hydroxy-4'-(2-hydroxyethoxy)-2-methylpropiophenone (224 g/mole) was added (0.2% m/v) and the solution was mixed until the solids were fully dissolved.

2.3. Preparation of Hydrogel Coating on Capillary

The production of a hydrogel coating on the glass capillary is a two-step process that can be performed at room temperature. The first step is the functionalization of a borosilicate glass capillary tube with methacrylate groups to allow for stronger covalent bonds between the hydrogel and the tube. The tube is subsequently coated with a hydrogel precursor solution and exposed to UV light to form the hydrogel.

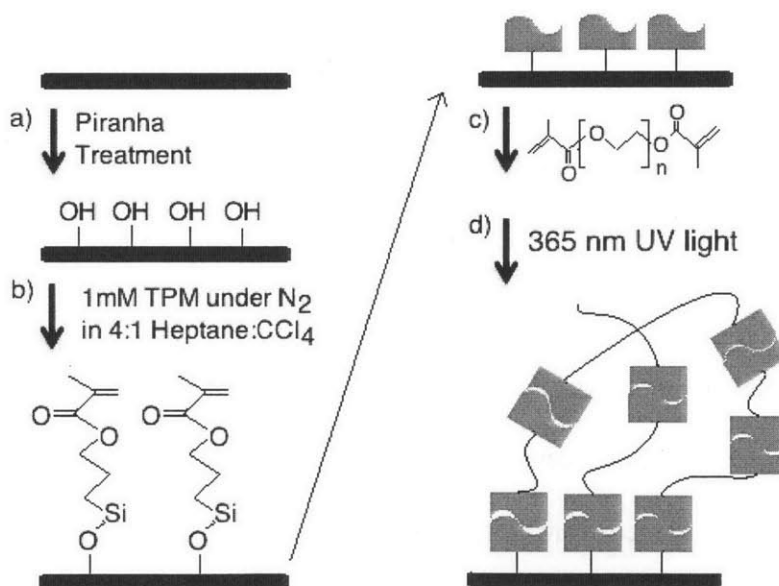**Figure 2.** a) capillary tubes are treated with piranha solution to hydroxylate the surface b) capillary tubes are functionalized with methacrylate groups using TPM c) poly (ethylene glycol)- dimethacrylate polymer chains are introduced d) exposure to UV light starts a photo-polymerization process that allows the methacrylate end groups of the polymer chains to bond to the surface and crosslink with each other

Capillary tubes with outer diameters of 150μm were first treated with a piranha solution to remove organic residues and hydroxylate the surface. The solution was created from a 3:1 mixture of 80% sulfuric acid to 30% hydrogen peroxide. The tubes were submerged in the solution for 10 minutes, washed with DI water, and dried with nitrogen gas.

The tubes were then treated with 1mM-3-(trichlorosilyl) propyl methacrylate (TPM) in order to add methacrylate end groups. The tubes were added to a 4:1 ratio of heptane and carbon tetrachloride. TPM was introduced under nitrogen at 0.1644μl/mL of the total solution. The solution was allowed to stir for 10 minutes. The tubes were washed with heptane, acetone and DI water.

A glass capillary mold with an inner diameter of 400 μm was used to constrain the hydrogel coating over the capillary tube. The hydrogel precursor solution then filled into the empty space through capillary action. The mold was exposed to 365 nm UV light for approximately 30s for each centimeter in length. Coated capillary tubes were stored in DI water at room temperature until use.

2.4. Gel Dependence on PEG MW and % PEG

Hydrogel precursor solutions of varying concentrations and molecular weights were synthesized according to Section 2.2. 0.2 g of each solution was added to a 1.5 mL eppendorf tube. The tube was exposed uniformly to UV light for 90s or until the solution gelled. The post-gelation weight was recorded and a hole was poked on the top of the eppendorf tube. The tubes were dried in vacuum for 2 days. The mass of the PEG (M_p), mass of the water (M_w), the relaxed gel mass (M_r) and the dry gel mass (M_d) for each sample was measured. The dry gel mass was assumed to be equivalent to the polymer mass (M_p). These measurements were used to calculate the mass swelling ratios, the polymer volume fraction,

the average molecular weight between crosslinks and the elastic modulus using equations (1)- (3).

2.5. Time Dependence of Swelling

Hydrogel coated capillaries were studied under an inverted optical microscope at different swelling states to determine the time evolution of swelling under free and constrained conditions. The capillary re-swelled in DI water in the unconstrained experiments. Constrained swelling experiments were conducted using a brain phantom composed of a 0.6% agarose gel with 0.005% w/v of Polybead@ polystyrene 6.0 μm microparticles. Small 1mm holes were drilled into the sides of 12-well cell culture plates and the agarose solution was gelled inside the wells. Hydrogel coated capillaries were immersed in DI water and allowed to swell to an equilibrium diameter (D_s). The capillary was dehydrated in a vacuum for 20 minutes and the diameter recorded (D_d). The dried capillary was then inserted into the agarose through the hole in the well plate as horizontally as possible to stay within the focus of the microscope. Images were taken at various time points. These images were used to determine an equation to describe the time dependence of swelling. Additionally, using ImageJ's Particle Image Velocimetry plug-in, the movement of the particles in the agarose solution was observed to generate a vector plot to show agarose and gel movement during different time intervals.

3. Results

3.1. Gel Dependence on PEG MW and % PEG

Four different molecular weights and three different mass percentages of PEG were studied. The swelling parameters as shown in Table 2 are the average of three determinations of the specimens. Some insolubility at the highest molecular weights (8000 g/mole) was observed. The hydrogel was difficult to cross-link at the lower mass percentages, and the gel was observed to be less 'gel-like' and more fluid.

Table 2

Summary of swelling parameters for different hydrogel formulations

MW	m/v %	Q_m	$v_{2,s}$	M_c^*
	5%	20.2±2.7	0.043±0.004	306±8
700 PEG-DA	10%	10.5±2.6	0.079±0.008	269±16
	20%	5.9±0.6	0.132±0.015	221±26
	5%	20.7±4.1	0.041±0.002	733±28
2000 PEG-DM	10%	10.1±1.4	0.082±0.011	514±90
	20%	7.6±0.9	0.105±0.002	523±14
	5%	18.9±10.8	0.046±0.005	1047±150
4000 PEG-DM	10%	12.2±1.6	0.069±0.009	909±163
	20%	5.9±0.3	0.132±0.002	425±36
	5%	46.7±10.8	0.020±0.005	3124±353
8000 PEG-DM	10%	13.3±1.5	0.063±0.003	1365±109
	20%	6.0±0.1	0.129±0.004	554±36

The swelling ratios are approximately the inverse of the mass percentages, which is consistent with expectations. The values for average molecular weight between crosslinks are shown in Figure 3. Two trends can be observed. First, an increase in polymer concentration leads to a decrease in the average molecular weight between crosslinks, which suggests an increase in crosslink density. Second, the average molecular weight between crosslinks increases linearly with the molecular weight of the original polymer. This relationship is less clear in hydrogels with higher percentages of PEG due to increased numbers of physical crosslinks. This form of

crosslinks include weak van der Waals' forces and entanglements, both of which are more significant at higher concentrations of polymer.
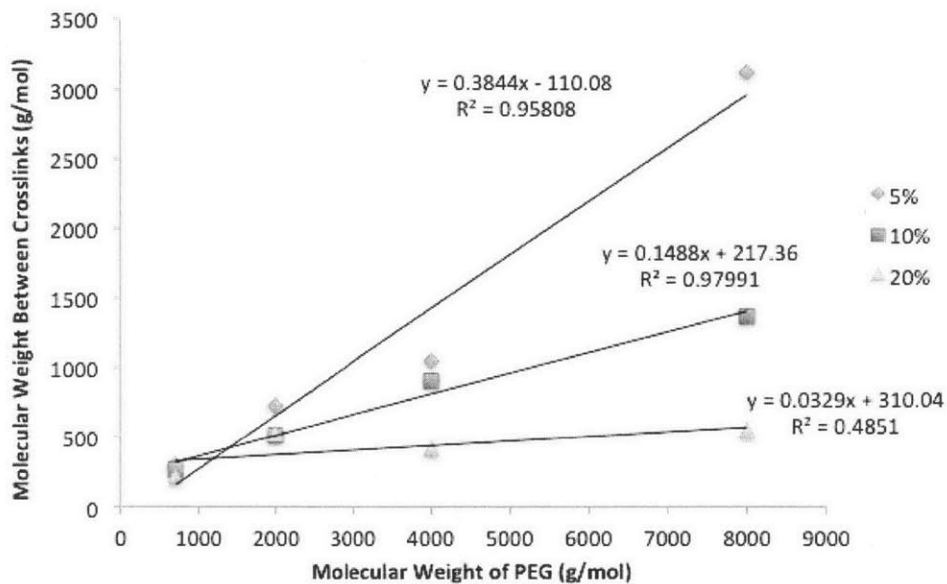
Figure 3. Increased polymer concentrations leads to increased crosslink densities. Increased molecular weights of PEG leads to increased molecular weight between crosslinks.

The elastic modulus for different hydrogels was calculated using equation (4). The unadjusted molecular weight between crosslinks values were used (Figure 4). The crosslink density decreases when the molecular weight between crosslinks increases, which leads to softer hydrogel with a smaller elastic modulus. This phenomenon is, however, not clear from the results shown. The modulus of the 20% PEG- 2000 gel is lower than expected and the modulus of the 5% PEG-4000 gel is higher than expected.
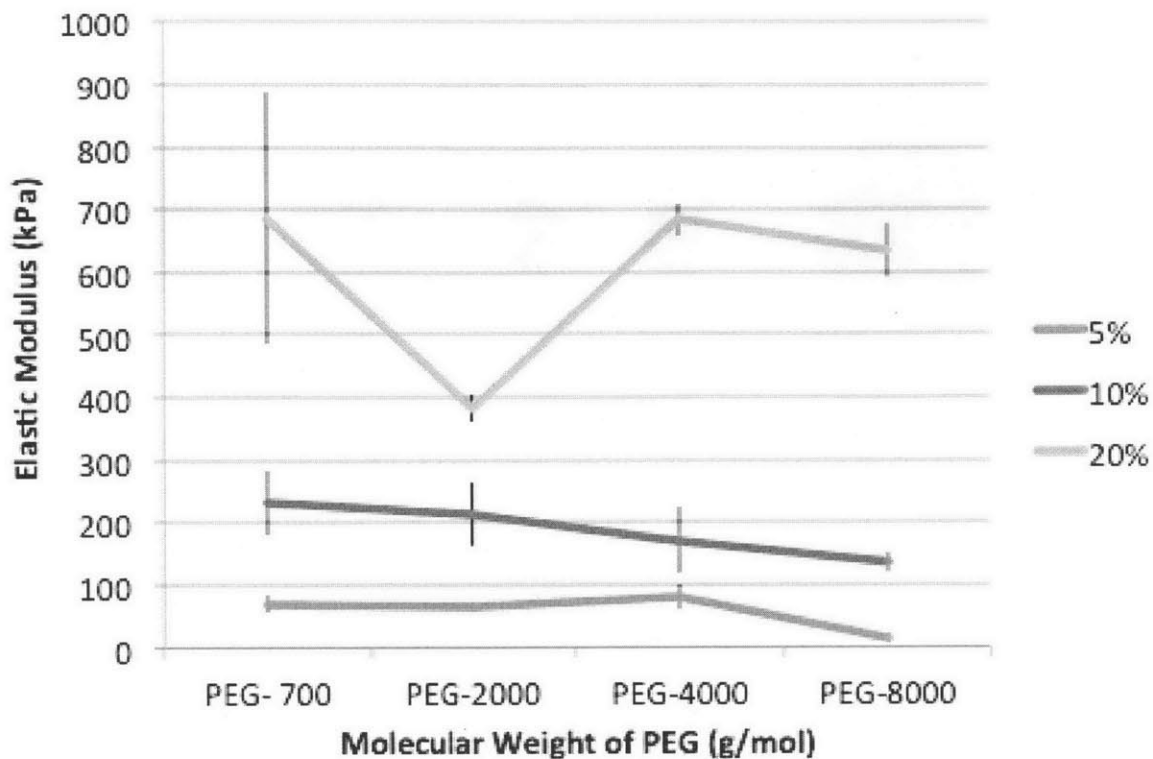
Figure 4. Estimated elastic modulus for different hydrogel formulations. Increasing the polymer concentration is an effective way to change the elastic modulus.

3.2. Swelling Ratio of Hydrogel-Coated Capillaries

A high degree of variability in the quality of the hydrogels was observed due to the difficulty in removing the hydrogel from the mold during the fabrication process. Part of the hydrogel coating often sheared off. Care was taken to use hydrogel-coated capillaries with no prominent defects for subsequent experiments. The diameter of the hydrogel-coated capillary was measured at different time points using Image J's 'Distance Between Polylines' plug-in to determine the swelling ratios from swelling and drying capillaries.
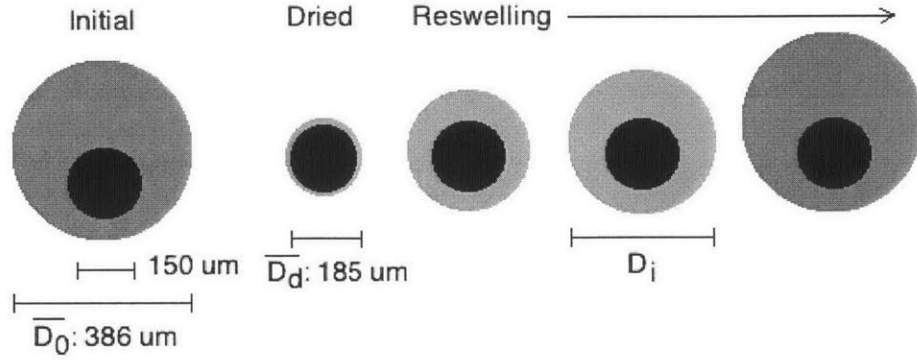
Figure 5. Capillary is not centered within the hydrogel after the fabrication process. The overall cross-section of the hydrogel is still assumed to be spherical due to the shape of the mold. During re-swelling, the side with a thinner layer of hydrogel reaches equilibrium first

The cross-sectional area (A_i) of the hydrogel at each time point was estimated using the total measured diameter (D_i) from ImageJ and the expected diameter of the capillary (D_c), which for these experiments were 150μm (Figure 5).

$$A_i = \pi \left[\left(\frac{D_i}{2} \right)^2 - \left(\frac{150 \mu m}{2} \right)^2 \right]$$ (6)

Once the cross-sectional area was determined, the swelling ratio was estimated using

$$Q_m = \frac{(A_t - A_d)\rho_w + A_d * \rho_p}{A_d * \rho_p}$$ (7)

where A_t is the cross-sectional area of a swollen gel at time t and A_d is the cross-sectional area of the dried gel. A_t is equal to A_0 for calculations of the initial swelling ratio, where A_0 is the initial diameter prior to drying out.

Table 3

Average parameters for hydrogel coated capillary (10%, 700 MW PEG-DA)

	Sample 1	Sample 2	Sample 3	Average
Initial Diameter* (μm)	390	389	381	386
Dry Diameter (μm)	188	178	189	185a
Initial Area (μm^2)	101,512	100,992	96,109	99,352
Dry Area (μm^2)	9,935	7,275	10,230	9,147
Swelling Ratio	9.2	12.4	9.4	10.4

*Diameter refers to the full diameter of the hydrogel- coated capillary

The swelling ratio[1] of the hydrogel on the capillary (10.4) is within range of the swelling ratio of the hydrogel alone (10.5) as shown in table 2 and 3. This suggests that having the hydrogel coated onto a capillary does not change the swelling parameters drastically.
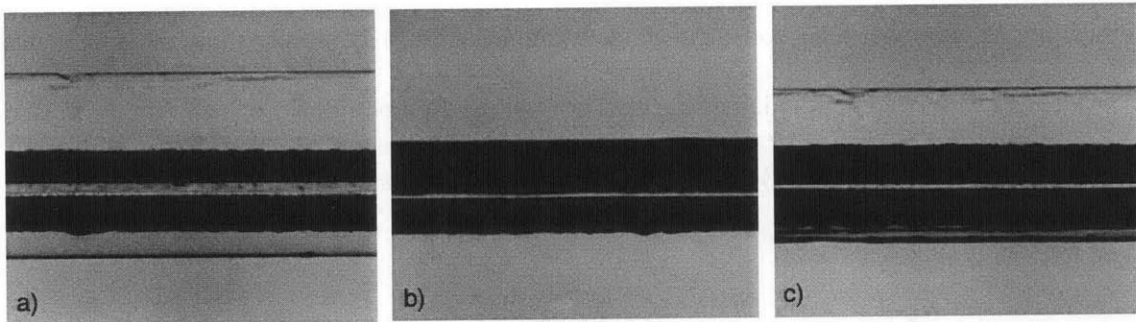
Figure 6. a) Initial swollen hydrogel at equilibrium, b) Dried hydrogel c) Swollen gel after 1 minute of re-swelling.

3.3. Time Dependence of Swelling

Insertion of a swollen hydrogel into the brain phantom caused shearing of the hydrogel (Figure 7). Dehydrating the hydrogel prior to insertion avoided this problem. Dehydrated hydrogels swelled after insertion into the brain phantom due to the agarose's high water content.

---

[1] To avoid confusion, the swelling ratio refers to the ratio of the initial gel mass to the dry gel mass. The re-swelling ratio refers to the ratio of gel mass after re-swelling to the dry gel mass.
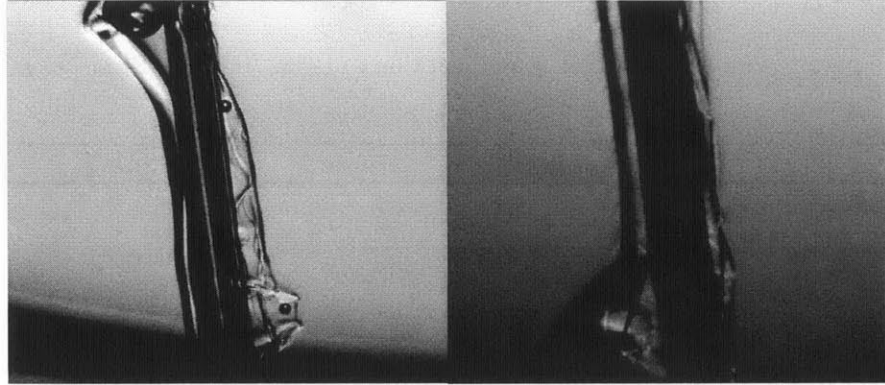
Figure 7. When the hydrogel is inserted into the brain phantom without dehydration, the hydrogel shears off and the coating is compromised.

The corresponding hydrogel cross-sections were calculated using equation (6) and the re-swelling ratios using equation (7). The resulting time course of swelling was fit using a power law equation. Figure 8 below compares the time courses for swelling in water and swelling in agarose. The constrained swelling in agarose is slower than the unconstrained process in water as expected. The gel had not yet reached equilibrium at the time the last data point was taken (~ one hour) for both swelling experiments.

Water: $y = 3.1562x^{0.0647}$
$R^2 = 0.91359$

Agarose: $y = 3.0539x^{0.0645}$
$R^2 = 0.96761$
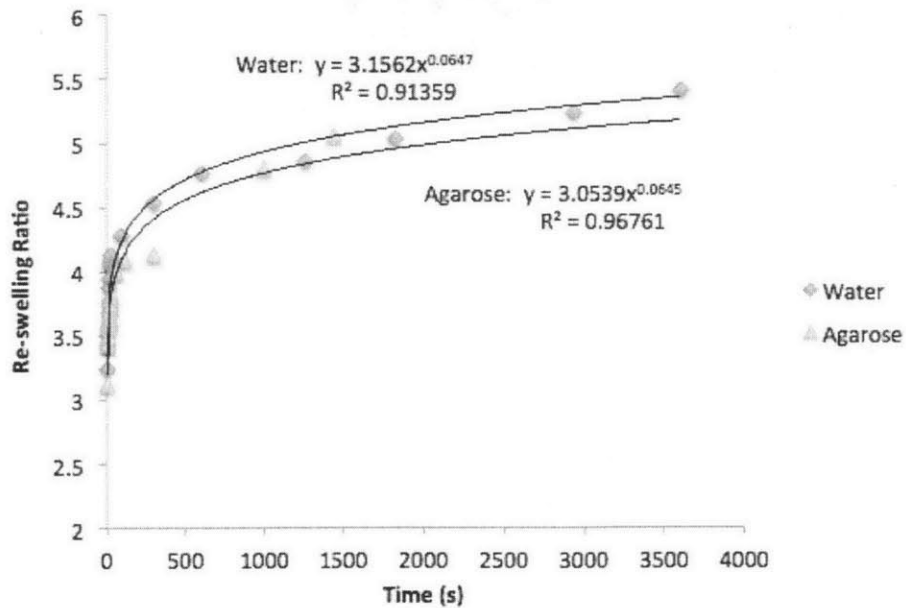
Figure 8. Time course for the swelling of a 10% 700 MW hydrogel coated capillary in water versus agarose

The time course experiment was repeated using 20%, 700 MW PEG- DA hydrogels. The re-swelling ratio levels off before 300 seconds, demonstrating that the hydrogel reached equilibrium (Figure 9) in both the water and agarose swelling experiments.

Figure 9. Time course for the swelling of 20% 700 MW hydrogel coated capillary in water versus agarose. The gel reached equilibrium around 125 seconds.

Figure 10 shows the swelling time course before the gel reached equilibrium. The power law fit has an exponent of 0.25-0.27 which is higher than the exponent from Figure 6 for the 10% gel (0.065). This suggests that swelling in the 20% gel occurs more rapidly than in the 10% gel. Figure 10 also confirms that swelling in agarose is slightly slower than the swelling in water.

Water: $y = 1.45x^{0.2753}$
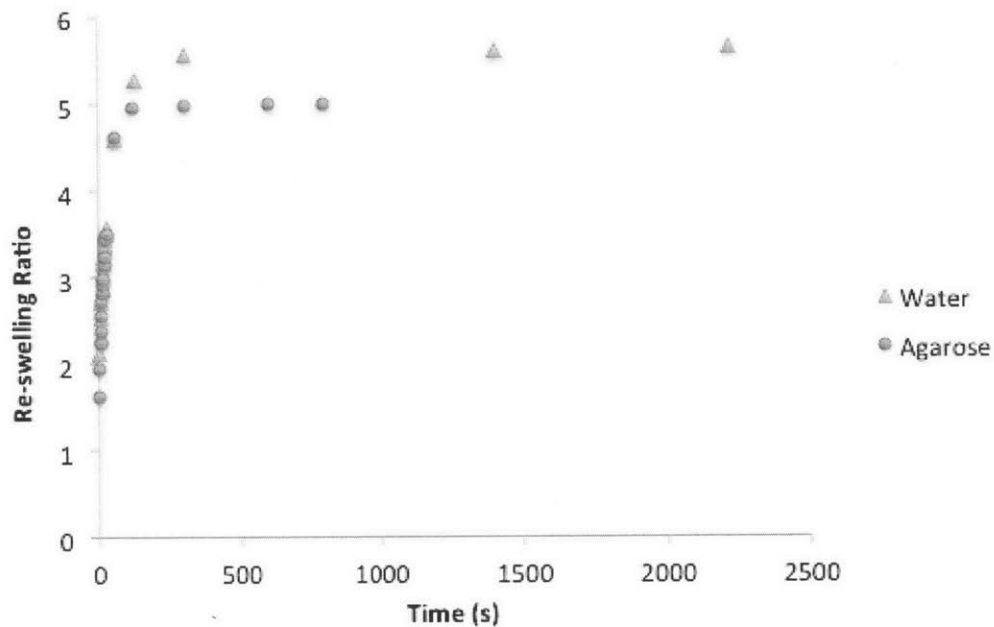$R^2 = 0.99432$

Agarose: $y = 1.5059x^{0.2523}$
$R^2 = 0.98321$
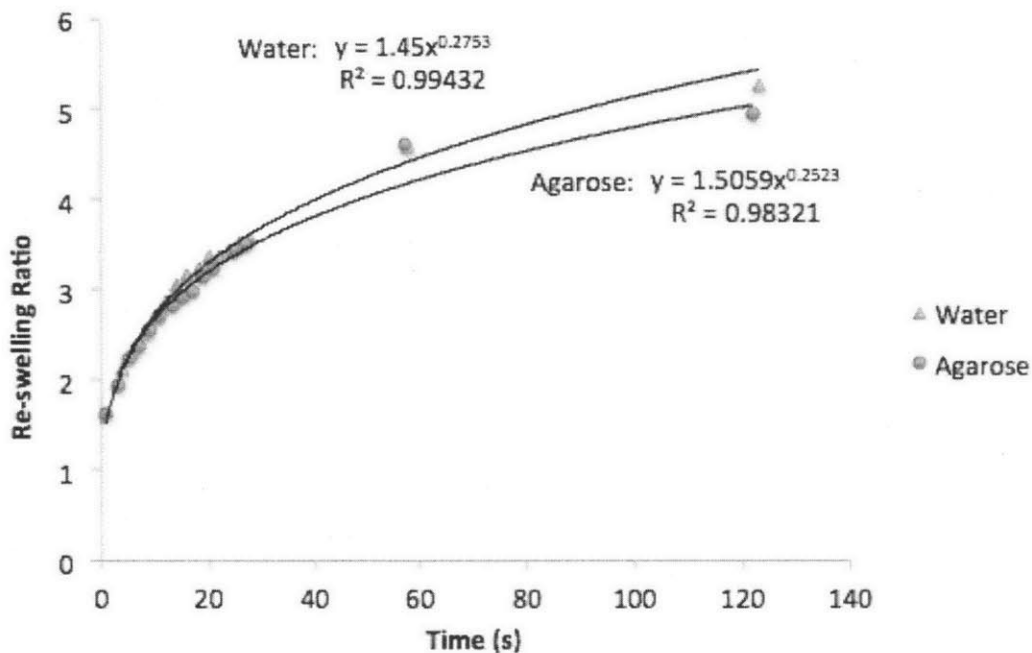
Figure 10. Time course for the swelling of 20% 700 MW hydrogel coated capillary in water versus agarose for the first 125 seconds before the gel reached equilibrium.

3.4. Vector Plot Observations

The effect of the hydrogel expansion on the agarose can be observed using Particle Image Velocimetry. The data presented in this section was for the gel shown in Figure 11a-b. Figure 11 shows a sample vector plot that shows the direction and magnitude of the agarose movement. The average displacement in the x and y directions are plotted in Figure 11c-h as a function of distance away from the capillary for different time intervals. The magnitude of the total displacement is also shown.

Positive x-displacement is defined as moving away from the capillary. Positive y-displacement is defined as moving down because the capillary was inserted in the downward direction. Negative x-axis values correspond to the agarose to the left of the capillary while the positive x-axis values correspond to the agarose on the right side.

The surrounding agarose moved in a similar direction as the capillary two seconds after implantation. The agarose shifted as if it was 'pulled' along, as indicated by the large displacements in the positive y-direction (Figure 11d). The figure also shows that the effects of implantation can be felt up to 2000 µm away. The agarose 'readjusted' and shifted upward to its undisturbed position as indicated by the large negative y displacements after 4 seconds (Figure 11e). The displacements decrease linearly as the distance from the capillary increases in both Figures 11d and 11e. In Figure 11f, the effect of both the agarose re-adjusting and the hydrogel expanding can be seen. The gel is still re-adjusting upwards although with smaller magnitudes than before on the right side of the capillary. The left side shows that the displacement is now decreasing exponentially with distance from the capillary, which is caused by the expansion of the hydrogel. Figure 11g shows that after 36 seconds, the bulk of the agarose stopped moving and all displacement was due to the expanding hydrogel. Small perturbations seen on the graphs for the right side of the capillary is due the expanding hydrogel pushing the capillary to the right side slightly. Similar phenomena can be seen from 126-296 seconds in Figure 11h.
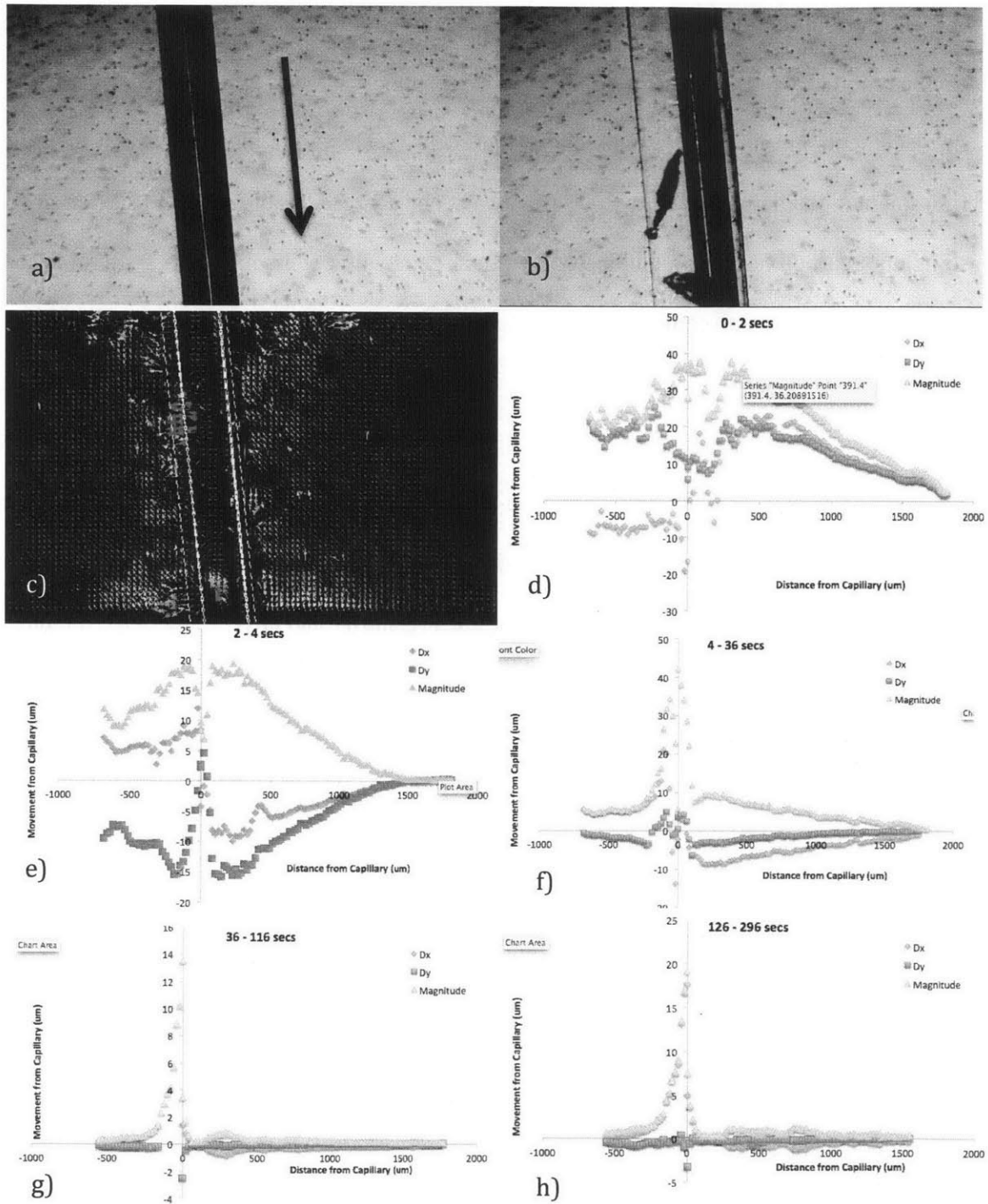
Figure 11. a) capillary showing direction of implantation b) capillary after 300 seconds of swelling in agarose c) sample vector plot for time interval of 2-4 seconds with white lines indicating the capillary and gel boundaries d) 0-2s: large y displacement values indicate agarose is moving along the direction of implantation e) 2-4s: large negative y displacement values indicate agarose is readjusting back to its initial position f) 4-36s: displacement exponentially decays on the left side due to hydrogel expansion while displacement linearly decreases on the right side due to agarose readjusting. g/h) bulk of agarose is at equilibrium; all movement is due to agarose expansion.

24

4. Discussion

4.1. Gel Dependence on PEG MW and % PEG

It was commonly reported in the literature that a recently cross-linked gel was allowed to swell in PBS for over 2 days to reach the equilibrium, swollen state[xi]. No additional swelling was detected in these experiments. The 10% and 20% gels experienced a loss in mass. This can likely be attributed to the small size of the hydrogel. The surface of the hydrogel began to dry out immediately upon exposure to open air, giving an inaccurate measure of the weight. The recently cross-linked state was considered to be the swollen state in calculations for $v_{2,s}$ to compensate. The relaxed state volume fraction ($v_{2,r}$) was calculated using the initial masses of PEG and water. This adjustment produces an over-estimation in elastic moduli calculations since less swelling was detected than most likely existed in actuality.

Elastic moduli calculated using adjusted molecular weight between crosslinks values were approximately an order of magnitude larger than those shown in Figure 4. Calculations using the unadjusted molecular weights produced elastic moduli values that were more consistent with those reported from previous literature[xii]. Bryant reported compressive moduli of 34-360kPa for 10-20% PEG-DM gels of MW 3400. It is not unexpected that the calculated results would be higher than those reported by Bryant as a result of the way the volume fractions were determined.

Figure 4 did not show clearly than an increase in MW of PEG leads to a decrease in elastic modulus as expected. This is because the expected trend exists within the same order of magnitude. The error bars show that values within one order of magnitude cannot accurately be distinguished. This error can be attributed to the small sample sizes used. Masses as low as 0.009g were measured. Values at this scale can be inaccurate so future hydrogel characterization experiments should use larger sample sizes. Figure 4 did show that

an increase in percentage of PEG leads to an increase in elastic modulus. Increasing the percentage of PEG from 5 to 20% was able to increase the elastic modulus by almost 2 orders of magnitude for the PEG-8000 gel.

4.2. Swelling Ratio of Hydrogel-Coated Capillaries

Drying out the hydrogel allowed the capillary to be inserted easily as expected. The brain phantom provided the water necessary for the hydrogel to return to its initial swollen state. Most hydrogel coatings over the capillary were uneven, as shown in Figure 6 and 11a. This makes it difficult to predict the effects of the cylindrical shape on the swelling. An even hydrogel coating will expand radially and along the length of the capillary as well.

Buckling (Figure 12) was observed in some samples as the hydrogel swelled due to the hydrogel being chemically tethered down to the capillary. Samples where this occurred were not used because it would cause uneven strain on the surrounding agarose. This was more likely to occur in samples that were left to dry for over a day.
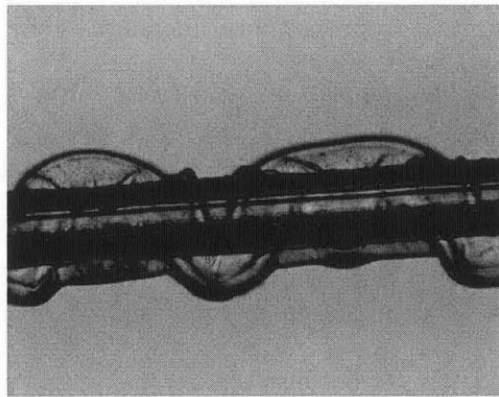

Figure 12. Buckling of the hydrogel occurred during swelling in some samples when the hydrogel dried for extended periods of time

4.3. Time Course of Hydrogel-Coated Capillaries

A power law fit assuming Fickian diffusion has the exponent of around 0.5. The fits for the swelling of 10% and 20% gels as shown in Figure 8 and 10 have exponents lower than 0.5. This "Less Fickian" behavior occurs when the water penetration rate is much lower than the polymer chain relaxation rate. Previous literature report power law fits only relevant for swelling below 60%[xiii]. The power law fit was able to describe swelling up to equilibrium in these experiments. This is most likely because the total hydrogel thickness is very thin (on the scale of μm) while most literature reports have used hydrogels on the scale of millimeters[xi].

The difference between swelling in agarose and water is very slight for both percentages of PEG, but both do show that swelling in agarose is slower, as expected. The equilibrium hydrogel state for the 20% gel in agarose was observed to be smaller than the equilibrium state of the gel in water. This implies that the hydrogel is slightly compressed as well, which matches hypotheses that the hydrogel will absorb some of the strain.

Experiments using the 20% hydrogels were able to reach equilibrium at around 2 minutes while the 10% hydrogels did not reach equilibrium within an hour. This can be explained by the difference in elastic moduli. Figure 4 showed that the elastic modulus for the 20% hydrogel is higher than that of the 10% hydrogel. A higher elastic modulus allows the 20% hydrogel to push more against the agarose, expand faster and reach equilibrium sooner. Further experiments are needed to determine when the 10% hydrogels will reach equilibrium.

Swelling in the brain will be slower than swelling in the brain phantom. The brain phantom is composed of 99.4% water while the brain's water content is generally accepted to be around 75%. Water from the brain will be less accessible to the hydrogel, which will slow

the swelling process. Mouse models will provide better insight into the swelling time course in brain tissue.

The rapid swelling of the hydrogel coating could prove to be problematic during implantation into brain tissue. Surgical implantation procedures require accuracy and precision so the implantation process is on the scale of minutes or more. This contrasts with the swelling of a hydrogel, which is capable of reaching almost 70% of its equilibrium state within 30 seconds. This could compromise the integrity of the hydrogel and cause more injury during implantation.

4.4. Vector Field Observations

Most of the strain from inserting the capillary occurred within the first four seconds as a result of the insertion. The surrounding agarose shifted in the direction of movement and then shifted backwards to readjust. The effects of this phenomenon could be felt up to 2000μm away. The effects of the hydrogel expansion only affected the regions nearest to the capillary (within 250μm).

One problem during the collection of the data was that in order to ensure that the inserted hydrogel was in focus, an initial portion of the capillary was inserted slightly. Any hydrogel on the capillary tip swelled immediately. This soft hydrogel tip caused less tearing of the agarose during implantation, but exacerbated the 'pulling' phenomenon, which resonated more throughout the gel.

5. Conclusion

PEG-DA and PEG-DM hydrogel coated capillaries were synthesized and characterized. The properties of the hydrogels were varied by altering the percentage and molecular weight of PEG. Calculated elastic moduli values ranged from 13kPa to 687 kPa and are similar to that of the brain (6kPa). Dehydration of the hydrogels

allowed the capillary to be easily inserted into brain phantoms. Nearly instantaneously, the hydrogel began to imbibe water and swell. Hydrogels with higher moduli were observed to swell faster in both water and agarose. The 20% hydrogels reached equilibrium within 300 seconds while the 10% hydrogels did not reach equilibrium within an hour. Swelling in agarose was slower than swelling in water and reached a smaller equilibrium state. In the future, time course experiments need to be conducted with more hydrogel formulations to confirm the trends observed. Mouse models can be used to more accurately determine swelling behavior in brain tissue. A mechanism needs to be developed to produce even hydrogel coatings. This would normalize the results more effectively since it is uncertain how much data variability is due to hydrogel variability. Additional tests are needed to determine the ideal thickness of the coating such that it provides enough mechanical compatibility without compromising device function.

6. Acknowledgements

References

[i] Miocinovic S, Somayajula S, Chitnis S, Vitek JL, History, applications, and mechanisms of deep brain stimulation. *JAMA Neurol.* 2013 Feb; 70(2) 163-71

[ii] Polikov V.S., Tresco, P.A., Reichert, W. M. Response of brain tissue to chronically implanted neural electrodes. Journal of Neuroscience Methods. 2005 Oct; 148 (1), 1-18

[iii] Subbaroyan, J., Martin, D.C., and Daryl R. Kipke. A finite-element model of the mechanical effects of implantable microelectrodes in the cerebral cortex. J. Neural Eng. 2005(2), 103-113

[iv] Peppas, N.A., Huang, Y., Torres-Lugo, M., Ward, J.H., and J.Zhang, Physicochemical Foundations and Structural Design of Hydrogels in Medicine and Biology, Ann. Rev. Biomed. Eng. 2000. 02: 9-29

[v] Dai, X., Chen, X., Yang,L., Foster, S., Coury, AJ., and Thomas H. Jozefiak. Free radical polymerization of poly(ethylene glycol) diacrylate macromers: Impact of macromere hydrophobicity and initator chemistry on polymerization efficiency. Acta Biomaterialia, 2011, 1965-1972

[vi] Peppas, N.A, Merrill, E.W. Crosslinked poly(vinyl alcohol) hydrogels as swollen elastic networks. J. Appl. Polym. Sci., 21 (1977), pp. 1763-1770

[vii] Lin, HQ, Kai T, Freeman BD, Kalakkunnath S, Kalika DS. The effect of cross-linking on gas permeability in cross-linked poly(ethylene glycol diacrylate). Macromolecules. 2005;38(20):83181-8393

[viii] Merrill, E.W., Dennison, K.A, Sung, C. Partitioning and diffusion of solutes in hydrogels of poly(ethylene oxide). Biomaterials. 1993; 14(15): 1117-26

[ix] Silliman, JE, Network Hydrogel Polymers for Application to HemoDialysis, (Doctoral dissertation). MIT 1972

[x] Peppas, N.A., et al., Hydrogels in pharmaceutical formulations. European Journal of Pharmaceutics and Biopharmaceutics, 2000. 50(1): p. 27-46

[xi] Datta, A. Characterization of Polyethylene glycol hydrogels for Biomedical Applications. (Doctoral dissertation), Louisiana State University. 2007

[xii] Bryant, S.J. and K.S. Anseth, Hydrogel properties influence ECM production by chondrocytes photoencapsulated in poly(ethylene glycol) hydrogels. J Biomed Mater Res, 2002. 59(1): p. 63-72

[xiii] Ganji, F. Vasheghani-Farahani, S. and Ebrahim Vasheghani-Farahani. Theoretical Description of Hydrogel Swelling: A Review, Iranian Polymer Journal, 19(50, 2010, 375-398